Exploring UAS imaging modalities for precision agriculture: predicting table beet root yield and estimating disease severity using multispectral, hyperspectral, and LiDAR sensing

Mohammad S. Saif*[a], Robert Chancia[a], Sean P. Murphy[b], Sarah Pethybridge[b] and Jan van Aardt[a]
[a] Chester F. Carlson Center for Imaging Science, Rochester Institute of Technology, Rochester, NY USA 14623;
[b] Plant Pathology & Plant-Microbe Biology Section, School of Integrative Plant Science, Cornell AgriTech, Cornell University, Geneva, NY USA 14456;
* Correspondence: ms4667@rit.edu

ABSTRACT

Unmanned aerial systems (UAS) have gained popularity in precision agriculture research due to their relevant payloads, high spatial/spectral resolution, and ease of data acquisition. These systems come equipped with various imaging technologies to support crop monitoring and management. However, there remains a need to evaluate the performance of various imaging systems in the context of precision agriculture. Here we explore and compare the capabilities of multispectral (MSI), hyperspectral (HSI), and light detection and ranging (LiDAR) sensing systems to predict table beet root yield and estimate *Cercospora* Leaf Spot (CLS) disease severity. Our research was conducted at Cornell AgriTech in Geneva, NY, during the 2021 and 2022 growing seasons. Data were collected via a MicaSense five-band multispectral sensor, Headwall Nano hyperspectral sensor (272 bands; visible-near-infrared (VNIR) range), and Velodyne VLP-16 LiDAR for structural information. These data were captured at various stages of the crop growth cycle. We developed end-of-season table beet root yield models (best performing model had an $R^2_{test} = 0.82$ and $MAPE_{test} = 15.6\%$) by evaluating their performance using both individual sensor data and combinations of sensor data. CLS disease severity estimation models simultaneously were developed utilizing both multispectral and hyperspectral sensors, incorporating vegetation indices and texture metrics. Our findings highlight the respective strengths and limitations of each sensor system. While hyperspectral imagery provided marginal improvements in yield prediction, multispectral imagery offered comparable results with simpler data handling and higher spatial resolution. For disease severity estimation, multispectral imagery ($R^2_{test} = 0.90$ and $RMSE_{test} = 7.18$ %) outperformed hyperspectral data ($R^2_{test} = 0.87$ and $RMSE_{test} = 10.1$ %). Additionally, structure-from-motion (SfM)-derived structural metrics contributed more to yield estimation when compared to LiDAR data. This study builds upon our previous work on disease severity assessment and incorporates key findings from our ongoing yield estimation research. We ultimately demonstrated that reliable models for both yield prediction and disease severity estimation can be achieved using multispectral imagery alone, by providing a comprehensive comparison of sensor modalities. This highlights the practicality and cost-effectiveness of MSI for operational deployment. These insights support the informed selection of UAS imaging systems, contributing to optimized crop management, enhanced productivity, and sustainable agricultural practices.

Keywords: UAS, Multispectral, Hyperspectral, LiDAR, Precision Agriculture, Machine Learning, Sensor Comparison

1. INTRODUCTION

The application of unmanned aerial systems (UAS) in precision agriculture has garnered significant research interest in recent years due to the ability of UAS to deliver high-resolution, timely data with minimal labor input[1]. While much of the existing UAS-based research has focused on grain crops[2], there remains a notable gap in studies addressing specialty crops, such as table beets, which are gaining popularity owing to their nutritional benefits[3] and increasing consumer demand[4]. The only relevant study for table beet root yield estimation using multispectral imagery was performed by Chancia et al.[5], who achieved an $R^2 = 0.89$, while our previous study[6] using hyperspectral images achieved a top $R^2 = 0.90$. Both of these studies relied heavily on spectral information, yet it has been shown that structural information, extracted from structure-from-motion (SfM)[7] or LiDAR[8], could improve yield estimation.

Concurrently, UAS-based disease severity assessments have gained traction, particularly for *Cercospora* Leaf Spot (CLS) in beet crops. Görlich et al. [9] employed UAS RGB imagery to segment CLS-affected regions in sugar beets, achieving an

Algorithms, Technologies, and Applications for Multispectral and Hyperspectral Imaging XXXI, edited by Miguel Velez-Reyes, David W. Messinger, Proc. of SPIE Vol. 13455, 1345509 · 2025 Published bySPIE · 0277-786X · doi: 10.1117/12.3054031

F1 score of 44.48. Similarly, Yamati et al. [10] utilized UAS-based CNN models to classify disease severity levels, reporting an accuracy of 0.64. Barreto et al. [11], in turn, demonstrated that multispectral imagery can predict CLS severity with an R^2 of 0.87. Our prior research also highlighted the efficacy of multispectral imagery in estimating CLS severity in table beets, incorporating both spectral and textural features[12]. However, these studies largely emphasized single-sensor systems and did not extend their analysis to multiple sensing modalities.

Despite the demonstrated success of UAS-based sensing in estimating both yield and disease severity, a comprehensive evaluation of how various UAS sensor systems, specifically multispectral, hyperspectral, and LiDAR, compare across different agricultural variables within the same crop, is lacking. Furthermore, there is limited exploration of how these systems perform when applied to both disease severity assessment and yield estimation in tandem.

We address this gap by systematically comparing the performance of multispectral (MSI), hyperspectral (HSI), and LiDAR data for two key applications in table beet production, namely harvest root yield prediction and CLS disease severity estimation. Specifically, for yield estimation, we integrate results from our recent multi-season trials, incorporating spectral, structural, and meteorological data, and evaluate sensor performance across growing stages. While detailed methodology for root yield prediction will be presented in a forthcoming publication, this paper focuses on the comparative sensor performance results. Additionally, for disease severity assessment, we extend our prior work by developing new models using hyperspectral imagery, following a consistent feature extraction and modeling pipeline, as previously applied to multispectral data[12]. Our objective is to provide a holistic evaluation of sensor capabilities for precision agriculture applications in table beet, offering insights into optimal sensor selection for specific crop monitoring tasks.

2. METHODS

Field Trials

The table beet field trials were conducted at the Cornell AgriTech farm in Geneva, NY, during the 2021 and 2022 growing seasons. Specific plots within the same field were designated for distinct purposes: some for end-of-season beet root yield estimation, and others for *Cercospora* Leaf Spot (CLS) disease severity assessment. CLS severity evaluations were performed at five intervals throughout the growing season to capture disease progression. Detailed information on the disease assessment protocol is available in Saif et al. [12].

Unmanned Aerial System

A DJI Matrice 600 drone, equipped with different sensors, were used for this study. Here we focus specifically on the MSI, HSI, and LiDAR data (Table 1).

Table 1. Sensor configurations of the three different imaging systems used in the study.

	Multispectral	**Hyperspectral**	**LiDAR**
Sensor	MicaSense Rededge-M	Headwall Nano	Velodyne VLP 16
Number of spectral bands	5	272	1
Wavelength (nm)	475, 560, 668, 717, 840	400 – 1000	905
Flight Configuration			
Flight altitude (m)	15	45	15
Orthomosaic GSD (cm)	1	3	1 (CHM)

Harvest yield prediction

A series of Gaussian Process Regression (GPR)[13] models were developed to estimate table beet root yield using a combination of meteorological, spectral, and structural features. Spectral features were extracted from the five-band multispectral imagery, while structural features, specifically canopy volume estimates, were derived using SfM techniques

applied to the same multispectral dataset. Similarly, hyperspectral imagery provided high-dimensional spectral information, which was reduced via principal component analysis (PCA) to retain the most informative components, while structural metrics (canopy volume estimates) were obtained from LiDAR-derived canopy height models.

Three independent models were trained: (1) a model combining multispectral spectral features with SfM-derived structural data, (2) a model integrating hyperspectral spectral features with LiDAR structural information, and (3) cross-combination models with one incorporating hyperspectral spectral data with multispectral SfM structural features, and another utilizing multispectral spectral data alongside LiDAR-derived structural features. In all models, meteorological variables, such as growing degree days (GDD) [14], GDD at harvest ($GDD_{harvest}$), cumulative evapotranspiration (EVAP) [15], and EVAP at harvest ($EVAP_{harvest}$) were included to account for environmental conditions.

This framework facilitated a comparative evaluation of the predictive contributions of each sensor modality, both individually and in combination, highlighting their respective strengths in yield estimation. Specific spectral features from the multispectral imagery included the mean of green normalized difference vegetation index (GNDVI)[16], transformed chlorophyll absorption ratio index (TCARI)[17], and the green reflectance band. The first three principal components were utilized in the case of the hyperspectral data. A detailed description of the data preprocessing steps, feature extraction procedures, and model optimization techniques will be presented in a forthcoming publication, currently under preparation.

CLS Disease Severity Estimation

Spectral features, including various vegetation indices, and spatial features derived from texture metrics[18], were extracted from the imagery to capture canopy characteristics related to disease. We employed a two-stage feature selection pipeline, combining filter-based methods to reduce dimensionality and wrapper-based methods to refine feature subsets relevant to model performance, to optimize model inputs. These selected features subsequently were used to train machine learning models, specifically random forest regressors, with model outputs validated against expert-assessed field CLS severity (%).

In our earlier work[12] we detailed this process for multispectral imagery, where the renormalized difference vegetation index (RDVI)[19], skewness, and the near-infrared texture homogeneity coefficient of variation emerged as key features. In this study we applied the same methodology to the hyperspectral imagery to enable direct comparison between sensor modalities. For hyperspectral data, the algorithm identified the modified chlorophyll absorption ratio index-2 (MCARI2)[20] skewness, the 721 nm texture homogeneity coefficient of variation, 741 nm texture homogeneity kurtosis, and 761 nm texture dissimilarity skewness as the most informative features for disease severity estimation.

3. RESULTS

The scatter plots illustrating the model predictions versus actual root yield for test data set across various sensor combinations are shown in Figure 1 , while Table 2 shows the corresponding performance metrics summarized for each sensor combination. All sensor combinations were able to predict root yield at harvest across a wide range of values.

However, a closer examination of the numerical results highlights the subtle difference in model performance. Specifically, the combination of hyperspectral with SfM-derived canopy volume estimates exhibits the highest predictive accuracy, reflected in slightly better R^2 and RMSE values when compared to the other models. This suggests that hyperspectral and SfM-derived features provide marginal improvement to its multispectral and LiDAR counterpart with regards to harvest root yield estimation.

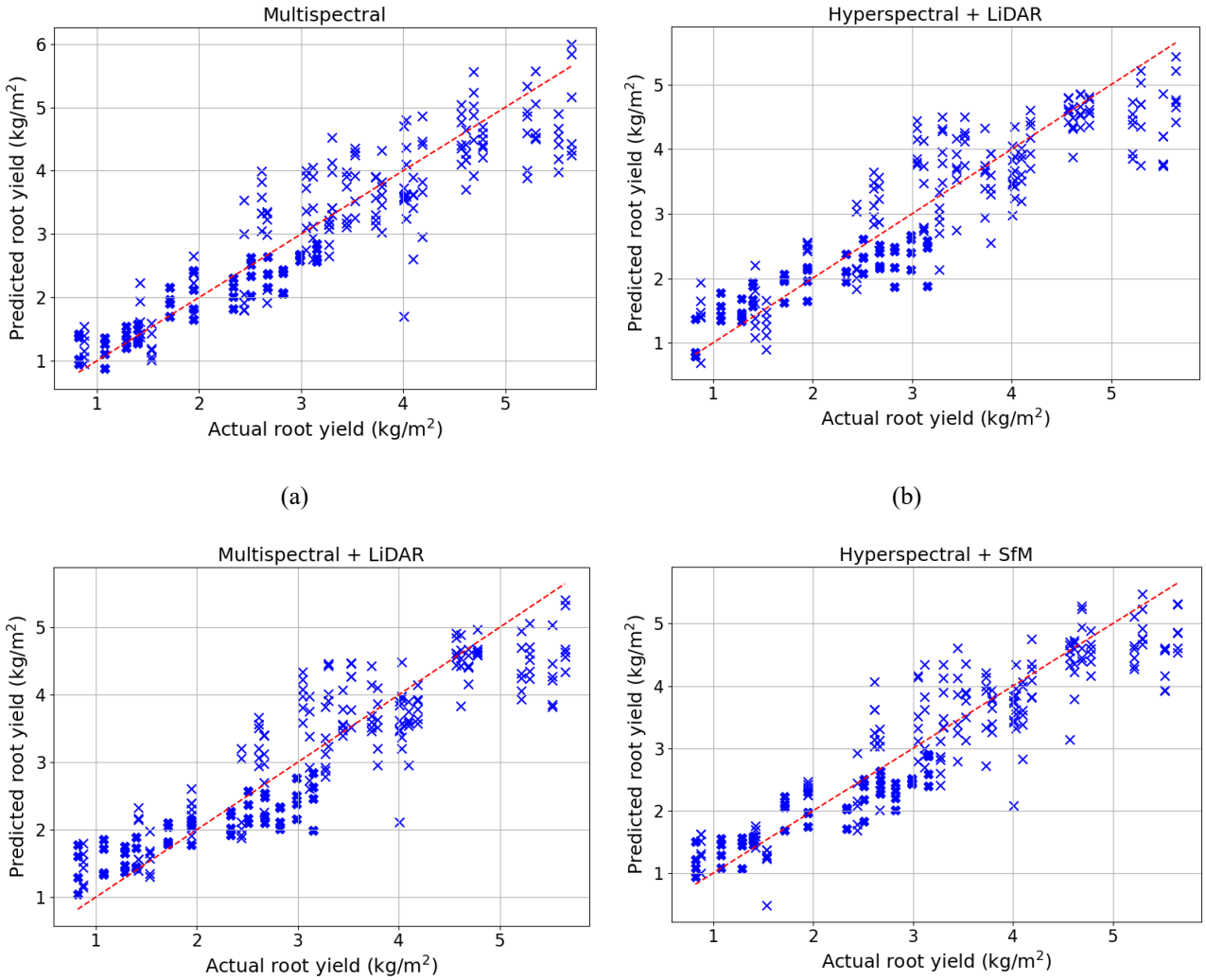

Figure 1. Predicted versus actual table beet root yield (kg/m²) for various sensor combinations across the 2021 and 2022 seasons. (a) Multispectral imagery with structure-from-motion (SfM)-derived structural features, (b) Hyperspectral imagery combined with LiDAR structural features, (c) Multispectral imagery combined with LiDAR structural features, and (d) Hyperspectral imagery with SfM-derived structural features. The red dashed line represents the 1:1 line, indicating perfect agreement between predicted and actual yields.

Table 2. Table beet root yield estimation performance for various sensor combinations.

	Multispectral + SfM	**Hyperspectral + LiDAR**	**Multispectral + LiDAR**	**Hyperspectral + SfM**
R^2_{Train} / $RMSE_{Train}$ (kg/m^2)	0.88 / 0.46	0.82 / 0.55	0.81 / 0.57	0.88 / 0.46
R^2_{Test} / $RMSE_{Test}$ (kg/m^2)	**0.81 / 0.58**	**0.79 / 0.61**	**0.79 / 0.60**	**0.82 / 0.56**

Similarly, Figure 2 shows the relationship between the best model performance of CLS disease severity using multispectral and hyperspectral systems, while Table 3 shows the performance for each system. Again, both systems were able to predict DS with reasonable accuracy; however, the multispectral system in this scenario exhibited better accuracy, while the hyperspectral system showed an inclination to saturate especially at high disease severity.

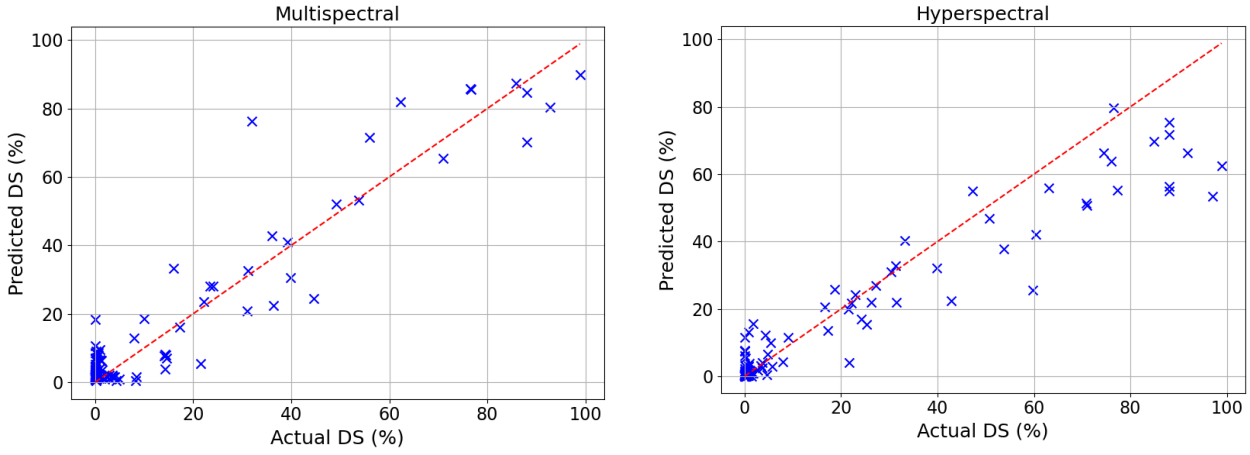

(a) (b)

Figure 2. Predicted versus actual *Cercospora* leaf spot severity (DS) (%) for table beet using (a) multispectral imagery and (b) hyperspectral imagery. The red dashed line represents the 1:1 line indicating perfect agreement between predicted and actual disease severity scores.

Table 3. Performance for *Cercospora* leaf spot severity estimation using the multispectral and hyperspectral sensors.

	Multispectral	**Hyperspectral**
R^2_{Train} / $RMSE_{Train}$ (%)	0.94 / 6.02	0.95 / 5.07
R^2_{Test} / $RMSE_{Test}$ (%)	**0.90 / 7.18**	**0.87 / 10.1**

4. DISCUSSION

The performance of our models for both harvest root yield prediction and CLS disease severity estimation align well with other studies in literature. Our yield prediction models demonstrated R^2 values comparable to, or exceeding, those reported in previous work. Similarly, while the hyperspectral-based model exhibited slightly poorer performance for disease severity estimation compared to multispectral imagery, it still outperformed many techniques documented in literature.

A key focus of this study was comparing sensor modalities to assess their strengths and limitations for specific agricultural applications. To provide additional context, we evaluated the signal-to-noise ratio (SNR) characteristics of both multispectral and hyperspectral systems (Figure 3). The analysis offers insight into how sensor-specific factors influenced model outcomes.

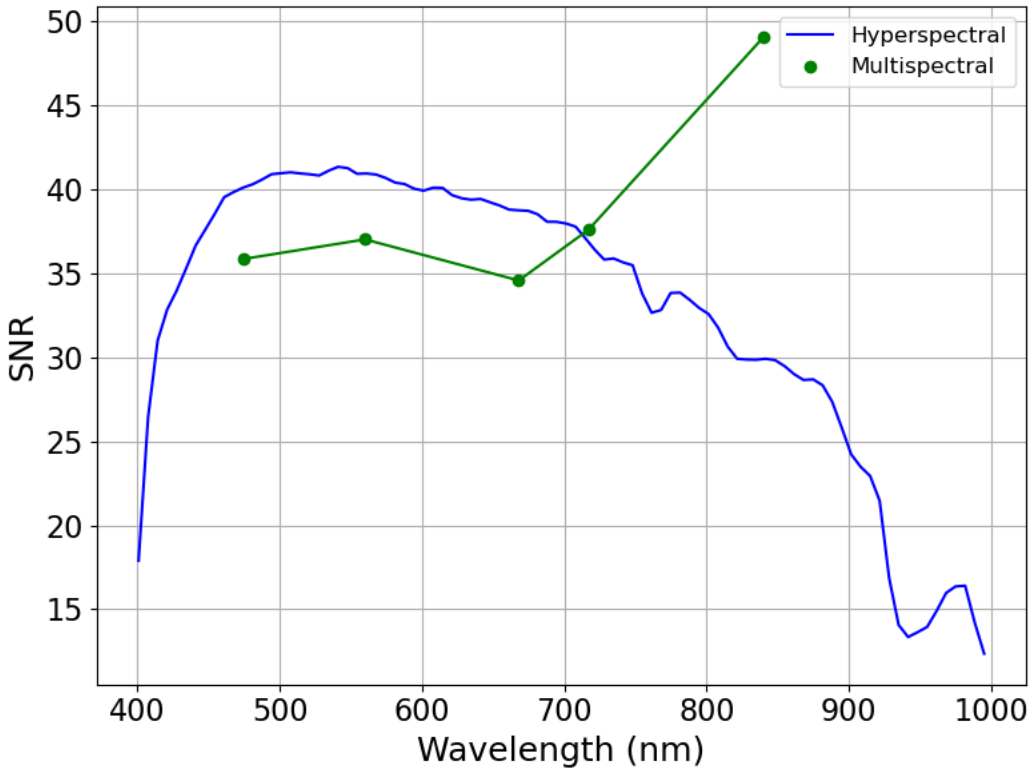

Figure 3. Scene noise estimation based on the signal-to-noise ratio (SNR) calculated from calibration panels. SNR was computed by dividing the mean reflectance value by the standard deviation of the reflectance values across all pixels within each panel. The plot compares SNR across wavelengths for both hyperspectral (blue line) and multispectral (green dots) sensors, illustrating the spectral noise characteristics of each system.

For root yield prediction, both multispectral and hyperspectral sensors yielded similar performance, with hyperspectral sensors showing a slight advantage. This is likely because yield estimation relied on the aggregate mean reflectance values across the scene and the broad spectral information was reduced via principal component analysis (PCA). In this scenario, neither the lower spatial resolution nor the lower SNR (particularly in the near-infrared region) of hyperspectral imagery significantly impacted model accuracy. The spatial resolution was less critical, as the model leveraged averaged canopy and structural metrics, rather than fine spatial details.

Conversely, for CLS disease severity estimation, the choice of sensor played a more decisive role. Disease estimation depended heavily on distribution-based metrics, such as vegetation index (VI) variability and texture features, both of which are sensitive to spatial resolution and image noise. The higher spatial resolution of multispectral imagery provided finer detail, enabling better capture of subtle variations in canopy health and disease lesion distribution. In contrast, the hyperspectral system's lower spatial resolution, coupled with its lower SNR in the NIR region, likely contributed to reduced performance. Moreover, hyperspectral data collection with push broom sensors posed additional challenges; orthorectification is more complex compared to frame-based scanners, while residual line jitter can introduce slight misregistration errors. These imperfections further complicated accurate texture and distribution feature extraction, particularly for higher disease severity levels where fine-scale discrimination is essential. The observed tendency of the hyperspectral model to saturate at high disease severity levels may also stem from these limitations. One potential mitigation strategy could involve stabilizing the hyperspectral sensor with a gimbal to minimize jitter effects.

On the structural side, our results indicate that SfM-derived canopy volume estimates contributed more effectively to yield prediction than LiDAR-based metrics. As shown in Figure 4, SfM consistently produced higher volume estimates when compared to LiDAR. This is likely due to LiDAR's enhanced penetrating capability when generating point clouds, leading to lower canopy volume estimation.

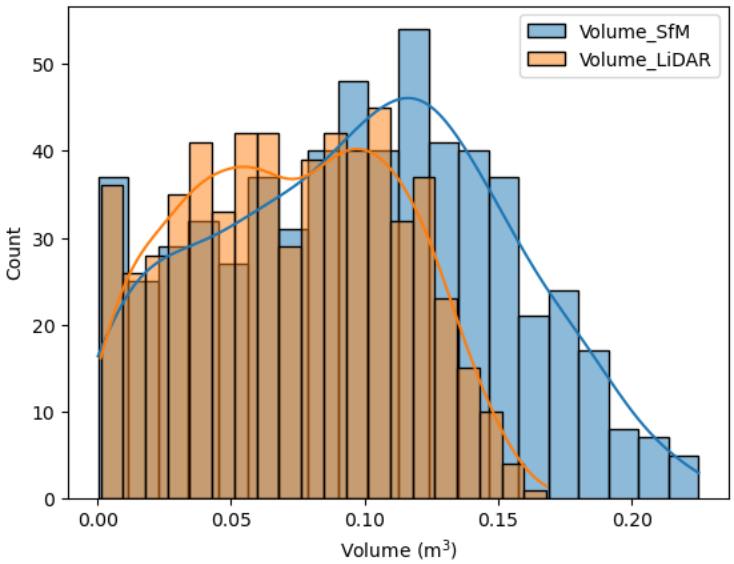

Figure 4. Histogram comparison of canopy volume estimates derived from structure-from-motion (SfM) and LiDAR data. The blue bars represent the volume distribution obtained from SfM-derived models, while the orange bars correspond to LiDAR-derived volumes. Smoothed kernel density estimation curves are overlaid to illustrate the distribution trends for each sensor modality, highlighting differences in volume estimation between the two methods.

5. CONCLUSION

This study presented a comprehensive evaluation of multiple UAS sensor modalities for two applications in table beet production: harvest root yield prediction and CLS disease severity estimation. Our results demonstrated that both multispectral and hyperspectral imagery, when combined with appropriate structural and meteorological features, achieved robust yield predictions across multiple seasons and growth stages. Hyperspectral imagery provided a marginal advantage in yield estimation due to its broader spectral coverage; however, the multispectral system delivered comparable performance, highlighting its practical utility given its operational simplicity.

For disease severity assessment, multispectral imagery outperformed hyperspectral data, primarily due to its superior spatial resolution and lower noise levels, which facilitated more accurate extraction of the distributions of vegetation indices and texture metrics. The hyperspectral system's lower spatial resolution and signal-to-noise ratio, coupled with inherent challenges in orthorectification, limited its effectiveness in capturing features critical for disease estimation. Additionally, our findings emphasized that structure-from-motion (SfM)-derived canopy volume estimates contributed more effectively to yield prediction than LiDAR-derived structural features.

Overall, this study provides valuable insights into the relative advantages and limitations of different UAS sensors for multi-parameter crop monitoring. Our comparative analysis offers practical guidance to researchers and practitioners aiming to optimize sensor deployment strategies in precision agriculture.

ACKNOWLEDGEMENTS

We gratefully acknowledge Nina Raqueno and Tim Bauch from the RIT drone team for their expertise and support in conducting the UAS flight campaigns. We also thank Imergen Rosario and Kedar Patki for their valuable assistance with field data collection. Special thanks to Pratibha Sharma for her contributions to the disease severity assessments.

REFERENCES

[1] Sishodia, R. P., Ray, R. L. and Singh, S. K., "Applications of Remote Sensing in Precision Agriculture: A Review," 19, Remote Sensing **12**(19), 3136 (2020).

[2] Tsouros, D. C., Bibi, S. and Sarigiannidis, P. G., "A Review on UAV-Based Applications for Precision Agriculture," 11, Information **10**(11), 349 (2019).

[3] Clifford, T., Howatson, G., West, D. J. and Stevenson, E. J., "The Potential Benefits of Red Beetroot Supplementation in Health and Disease," 4, Nutrients **7**(4), 2801–2822 (2015).

[4] Pethybridge, S. J., Kikkert, J. R., Hanson, L. E. and Nelson, S. C., "Challenges and Prospects for Building Resilient Disease Management Strategies and Tactics for the New York Table Beet Industry," 7, Agronomy **8**(7), 112 (2018).

[5] Chancia, R., van Aardt, J., Pethybridge, S., Cross, D. and Henderson, J., "Predicting Table Beet Root Yield with Multispectral UAS Imagery," 11, Remote Sensing **13**(11), 2180 (2021).

[6] Saif, M. S., Chancia, R., Pethybridge, S., Murphy, S. P., Hassanzadeh, A. and van Aardt, J., "Forecasting Table Beet Root Yield Using Spectral and Textural Features from Hyperspectral UAS Imagery," 3, Remote Sensing **15**(3), 794 (2023).

[7] Maimaitijiang, M., Sagan, V., Sidike, P., Maimaitiyiming, M., Hartling, S., Peterson, K. T., Maw, M. J. W., Shakoor, N., Mockler, T. and Fritschi, F. B., "Vegetation Index Weighted Canopy Volume Model (CVMVI) for soybean biomass estimation from Unmanned Aerial System-based RGB imagery," ISPRS Journal of Photogrammetry and Remote Sensing **151**, 27–41 (2019).

[8] Zhang, F., Hassanzadeh, A., Letendre, P., Kikkert, J., Pethybridge, S. and van Aardt, J., "Enhancing snap bean yield prediction through synergistic integration of UAS-Based LiDAR and multispectral imagery," Computers and Electronics in Agriculture **230**, 109923 (2025).

[9] Görlich, F., Marks, E., Mahlein, A.-K., König, K., Lottes, P. and Stachniss, C., "UAV-Based Classification of Cercospora Leaf Spot Using RGB Images," 2, Drones **5**(2), 34 (2021).

[10] Yamati, F. R. I., Barreto, A., Günder, M., Bauckhage, C. and Mahlein, A.-K., "Sensing the occurrence and dynamics of Cercospora leaf spot disease using UAV-supported image data and deep learning," Sugar Industry/Zuckerindustrie **147**(2), 79–86 (2022).

[11] Barreto, A., Ispizua Yamati, F. R., Varrelmann, M., Paulus, S. and Mahlein, A.-K., "Disease Incidence and Severity of Cercospora Leaf Spot in Sugar Beet Assessed by Multispectral Unmanned Aerial Images and Machine Learning," Plant Disease **107**(1), 188–200 (2023).

[12] Saif, M., Chancia, R., Sharma, P., Murphy, S. P., Pethybridge, S. J. and Aardt, J. van., "Estimation of Cercospora Leaf Spot Disease Severity in Table Beets from UAS Multispectral Images" (2025).

[13] Rasmussen, C. E. and Williams, C. K. I., [Gaussian processes for machine learning], MIT Press, Cambridge, Mass (2006).

[14] Pokhrel, A., Virk, S., Snider, J. L., Vellidis, G., Hand, L. C., Sintim, H. Y., Parkash, V., Chalise, D. P., Lee, J. M. and Byers, C., "Estimating yield-contributing physiological parameters of cotton using UAV-based imagery," Front. Plant Sci. **14** (2023).

[15] Cheng, M., Penuelas, J., McCabe, M. F., Atzberger, C., Jiao, X., Wu, W. and Jin, X., "Combining multi-indicators with machine-learning algorithms for maize yield early prediction at the county-level in China," Agricultural and Forest Meteorology **323**, 109057 (2022).

[16] Gitelson, A. A., Kaufman, Y. J. and Merzlyak, M. N., "Use of a green channel in remote sensing of global vegetation from EOS-MODIS," Remote Sensing of Environment **58**(3), 289–298 (1996).

[17] Haboudane, D., Miller, J. R., Tremblay, N., Zarco-Tejada, P. J. and Dextraze, L., "Integrated narrow-band vegetation indices for prediction of crop chlorophyll content for application to precision agriculture," Remote Sensing of Environment **81**(2), 416–426 (2002).

[18] Haralick, R. M., Shanmugam, K. and Dinstein, I., "Textural Features for Image Classification," IEEE Transactions on Systems, Man, and Cybernetics **SMC-3**(6), 610–621 (1973).

[19] Gitelson, A. and Merzlyak, M. N., "Spectral Reflectance Changes Associated with Autumn Senescence of Aesculus hippocastanum L. and Acer platanoides L. Leaves. Spectral Features and Relation to Chlorophyll Estimation," Journal of Plant Physiology **143**(3), 286–292 (1994).

[20] Haboudane, D., Miller, J. R., Pattey, E., Zarco-Tejada, P. J. and Strachan, I. B., "Hyperspectral vegetation indices and novel algorithms for predicting green LAI of crop canopies: Modeling and validation in the context of precision agriculture," Remote Sensing of Environment **90**(3), 337–352 (2004).